

**AFRL-PR-WP-TP-2006-238**

**PERFORMANCE IMPACTS DUE TO  
WAKE IN AXIAL-FLOW  
TURBOMACHINERY (Postprint)**

**T.J. Praisner, J.P. Clark, T.C. Nash, M.J. Rice, and E.A. Grover**



**SEPTEMBER 2006**

**Approved for public release; distribution is unlimited.**

**STINFO COPY**

**© 2006 ASME. The U.S. Government is joint author of the work and has the right to use, modify, reproduce, release, perform, display, or disclose the work.**

**PROPULSION DIRECTORATE  
AIR FORCE RESEARCH LABORATORY  
AIR FORCE MATERIEL COMMAND  
WRIGHT-PATTERSON AIR FORCE BASE, OH 45433-7251**

<b>REPORT DOCUMENTATION PAGE</b>				<i>Form Approved</i> OMB No. 0704-0188	
<p>The public reporting burden for this collection of information is estimated to average 1 hour per response, including the time for reviewing instructions, searching existing data sources, gathering and maintaining the data needed, and completing and reviewing the collection of information. Send comments regarding this burden estimate or any other aspect of this collection of information, including suggestions for reducing this burden, to Department of Defense, Washington Headquarters Services, Directorate for Information Operations and Reports (0704-0188), 1215 Jefferson Davis Highway, Suite 1204, Arlington, VA 22202-4302. Respondents should be aware that notwithstanding any other provision of law, no person shall be subject to any penalty for failing to comply with a collection of information if it does not display a currently valid OMB control number. <b>PLEASE DO NOT RETURN YOUR FORM TO THE ABOVE ADDRESS.</b></p>					
<b>1. REPORT DATE (DD-MM-YY)</b> September 2006		<b>2. REPORT TYPE</b> Journal paper postprint		<b>3. DATES COVERED (From - To)</b> 07/01/2005 – 09/15/2006	
<b>4. TITLE AND SUBTITLE</b> PERFORMANCE IMPACTS DUE TO WAKE IN AXIL-FLOW TURBOMACHINERY (Postprint)				<b>5a. CONTRACT NUMBER</b> IN HOUSE	
				<b>5b. GRANT NUMBER</b>	
				<b>5c. PROGRAM ELEMENT NUMBER</b> UNKNOWN	
<b>6. AUTHOR(S)</b> J.P. Clark (Turbine Engine Division, Turbine Branch (AFRL/PRTT)) T.J. Praisner, T.C. Nash, M.J. Rice, and E.A. Grover (United Technologies Corp.)				<b>5d. PROJECT NUMBER</b> UNKNOWN	
				<b>5e. TASK NUMBER</b> UNKNOWN	
				<b>5f. WORK UNIT NUMBER</b> UNKNOWN	
<b>7. PERFORMING ORGANIZATION NAME(S) AND ADDRESS(ES)</b>  Turbine Engine Division, Turbine Branch (AFRL/PRTT) Propulsion Directorate Air Force Research Laboratory, Air Force Materiel Command Wright-Patterson AFB, OH 45433-7251				<b>8. PERFORMING ORGANIZATION REPORT NUMBER</b>	
<div style="display: flex; justify-content: space-between;"> <div style="width: 45%;">           United Technologies Corporation Pratt &amp; Whitney Aerodynamics Group 400 Main St., M/S 169-29 East Hartford, CT 06108         </div> </div>					
<b>9. SPONSORING/MONITORING AGENCY NAME(S) AND ADDRESS(ES)</b>  Propulsion Directorate Air Force Research Laboratory Air Force Materiel Command Wright-Patterson AFB, OH 45433-7251				<b>10. SPONSORING/MONITORING AGENCY ACRONYM(S)</b> AFRL-PR-WP	
				<b>11. SPONSORING/MONITORING AGENCY REPORT NUMBER(S)</b> AFRL-PR-WP-TP-2006-238	
<b>12. DISTRIBUTION/AVAILABILITY STATEMENT</b> Approved for public release; distribution is unlimited.					
<b>13. SUPPLEMENTARY NOTES</b> © 2006 ASME. PAO case number AFRL/WS 06-1763, 14 July 2006. Printed in the Journal of Turbo Machinery by ASME, 2006. Best copy available.					
<b>14. ABSTRACT</b> Here, we demonstrate that the unsteady losses incurred as turbomachinery wakes mix in downstream rows are a function of the velocity ratio across the downstream row as calculated in the frame of reference of wake generation. Analytical and computational results, compared to measurements of wakes mixing under variable free-stream velocity conditions, reveal that wake-loss alteration is primarily a result of an inviscid dilation of the stream tubes that comprise the wake fluid. Further, simulations of wakes exposed to a range of turbomachinery-specific velocity ratios indicate that wake-loss augmentation caused by stream-tube dilation is significantly more pronounced than wake-loss reductions imparted by stream-tube contraction. It is demonstrated that wakes in turbines are dilated in the adjacent downstream row, whether it is a vane or a blade row, through a work extraction process that occurs in the wake-generation reference frame. Finally, comparisons between rig data and CFD simulations suggest that wake-mixing losses, enhanced by downstream rows, can contribute as much as 1.5 percent of lost efficiency in multi-stage LPTs.					
<b>15. SUBJECT TERMS</b> Turbines, Turbomachinery, Efficiency					
<b>16. SECURITY CLASSIFICATION OF:</b>			<b>17. LIMITATION OF ABSTRACT:</b> SAR	<b>18. NUMBER OF PAGES</b> 16	<b>19a. NAME OF RESPONSIBLE PERSON (Monitor)</b> John P. Clark <b>19b. TELEPHONE NUMBER (Include Area Code)</b> (937) 255-7152
<b>a. REPORT</b> Unclassified	<b>b. ABSTRACT</b> Unclassified	<b>c. THIS PAGE</b> Unclassified			

## PERFORMANCE IMPACTS DUE TO WAKE MIXING IN AXIAL-FLOW TURBOMACHINERY

T. J. Praisner<sup>1</sup>, J. P. Clark<sup>2</sup>, T. C. Nash<sup>1</sup>, M. J. Rice<sup>1</sup>, and E. A. Grover<sup>1</sup>

<sup>1</sup>Aerodynamics Group  
United Technologies Pratt & Whitney  
400 Main St., M/S 169-29  
East Hartford, CT 06108

<sup>2</sup>Turbine Branch, Turbine Engine Division  
Propulsion Directorate  
Air Force Research Laboratory  
1950 5th St., WPAFB, OH 45433

### ABSTRACT

One of the last loss mechanisms remaining to be quantified and correlated for inclusion in meanline predictive systems concerns the mixing of wakes across downstream airfoil rows. Here, we demonstrate that the unsteady losses incurred as turbomachinery wakes mix in downstream rows are a function of the velocity ratio across the downstream row as calculated in the frame of reference of wake generation. Analytical and computational results, compared to measurements of wakes mixing under variable free-stream velocity conditions, reveal that wake-loss modification is primarily a result of an inviscid dilation of the stream tubes that comprise the wake fluid. Further, simulations of wakes exposed to a range of turbomachinery-specific velocity ratios indicate that wake-loss *augmentation* caused by stream-tube dilation is significantly more pronounced than wake-loss *reductions* imparted by stream-tube contraction. It is demonstrated that wakes in turbines are diluted in the adjacent downstream row, whether it is a vane or a blade row, through a work extraction process that occurs in the wake-generation reference frame. Finally, comparisons between rig data and CFD simulations suggest that wake-mixing losses, enhanced by downstream rows, can contribute as much as 1.5 percent of lost efficiency in multi-stage low-pressure turbines.

### INTRODUCTION

The alteration of wake mixing caused by changes in free-stream velocity was first studied experimentally by Hill et al. [1] by exposing wakes to adverse pressure gradients within a diffuser. They found that when a wake is subjected to a range of adverse pressure gradients, the velocity profile across it could be dramatically altered, even to the point of local flow reversal along the wake centerline. Hill et al. also developed a model to predict the change in major wake-shape parameters for a range of favorable and adverse pressure gradients. However, the authors did not attempt to quantify the change in wake-mixing losses engendered by the changes in flow area.

Following closely the work of Hill et al. [1], Smith [2] considered the effects of wake stretching that occur in axial-flow compressors when the wake from one airfoil row enters a

downstream row. Smith used the term "wake recovery" to describe the reduction in wake-mixing loss that occurs as the wake fluid stream is contracted, or stretched, and extended the modeling of wakes to include this aspect. Similarly, Van Zante et al. [3] reported on their development of a new model to predict wake recovery in compressors. Utilizing a compressor rig, the authors also presented experimental data illustrating the effects of wake recovery on stage efficiency levels. They demonstrated good agreement between their model and the compressor-specific experimental data. The process of wake-loss attenuation engendered by stream-tube contraction in compressors is also covered conceptually by Greitzer et al. [4].

In his landmark paper concerning loss mechanisms in turbomachinery, Denton [5] discussed the effects of pressure gradients on wake mixing. Denton presented CFD-based results clearly demonstrating wake-loss augmentation caused by adverse pressure gradients (wake compression) and wake-loss attenuation, resulting from favorable pressure gradients (wake stretching). In the later part of his report, Denton presented mid-span entropy distributions from a time-accurate CFD simulation of a Low-Pressure Turbine (LPT). Denton concluded from his analysis of the simulation results that, primarily due to the disparate velocities on the suction and pressure sides of the simulated LPT airfoils, wakes undergo stretching in turbines and that losses would be reduced as a result. This conclusion contradicts the work of Smith [2] who reported "Wakes are amplified in turbines rather than attenuated [as in compressors]."

Hoffenberg and Sullivan [6] presented measured time-mean velocity and turbulence quantities of wakes passed through a variable-area diffuser. Although they did not report loss levels for their decelerated wakes, their results revealed significant dilation of the wake profiles with the application of adverse pressure gradients. The authors also performed numerical simulations of their experimental configuration. They concluded that while turbulence quantities within the decelerated wakes were matched reasonably well with both two-equation and Reynolds-stress turbulence models, the time-mean velocity profiles were very well duplicated by both classes of turbulence models.

Hodson and Dawes [7] provide a detailed discussion of the interpretation of measured turbine cascade losses with unsteady rod-generated wake passing. The authors presented pitch-wise experimental loss distributions of a cascade at midspan that revealed unexpectedly high losses incurred on the suction side of the passage in the core flow. This region of elevated loss was linked to unsteady losses associated with wakes convecting through the cascade passage. Hodson and Dawes reported that the mixing losses of the rod-generated wakes could be as much as doubled, relative to constant-area mixing, as the wakes passed through the cascade.

An assessment of wake mixing in turbine blade rows was presented by Rose and Harvey [8]. A wake-mixing-loss model was developed based on a canonical diffuser study such as that employed by Denton [5]. The model was validated by comparison to a single time-accurate simulation of a high-pressure turbine vane wake passing through a blade row. The authors reported that it was through a "differential work" mechanism that wake losses are attenuated in *both* turbines and compressors. So, while Smith [2] conjectured (in part based on his own thinking about the differential enthalpy extracted from the wake versus the freestream) that wake-loss modification trends are opposite in turbines and compressors, Rose and Harvey present the alternate view that the trend (attenuation) is the same, regardless of the direction the work takes as it crosses the control surface.

Recently, Praisner et al. [9] presented measured efficiency-versus-span data from a four-stage commercial LPT rig along with steady and time-accurate transitional CFD predictions. Their results demonstrated that the time-accurate simulation matched the data closely and provided the highest fidelity prediction. They also found that the steady simulation, conducted with a mixing-plane model, predicted significantly higher (less accurate) absolute levels of efficiency at all span-wise locations. It was suggested that the lower, more accurate results of the time-accurate simulation were primarily a result of increased losses in the core flow, due to wake-mixing effects not captured in the steady simulation.

There is consensus in literature that flow-area changes can attenuate or augment wake-mixing losses. Also, it is accepted that wake losses are attenuated in compressors. However, there is contradictory information in the open literature concerning the effect of downstream rows on wake-mixing losses in turbines. Moreover, there is limited turbomachinery-specific experimental data that directly addresses this phenomenon. So, the primary goals of the current work were to:

- Determine if turbine wake losses are attenuated or augmented in downstream rows.
- Isolate the salient geometric features that drive the alteration of wake mixing in turbines and compressors.
- Quantify the impact of wake mixing on turbine performance.

Where possible, existing experimental data was augmented by computational studies to address the aforementioned goals. However, wake-mixing loss variations due to downstream rows arise from unsteady effects and are relatively small (they will be shown to be of the order 10% of the loss of a typical LPT row). As a result, experimental evidence, such as that presented by Hodson and Dawes [7], of this small unsteady loss source is limited. Consequently, much of the work presented here is from analytical and computational work.

## NOMENCLATURE

### Latin:

$A$	Flow area
$ADP$	Aerodynamic Design Point
$b$	Wake half width
$C$	Chord
$H$	Wind tunnel height
$l$	Wake segment length
$LPT$	Low Pressure Turbine
$M$	Mach number
$MO$	Mixed-Out quantity
$n$	Normal direction
$P$	Pressure
$Re$	Reynolds number
$s$	Stream-wise distance
$ST$	Steady simulations
$V$	Velocity magnitude
$WVR$	Wake Velocity Ratio
$y$	Circumferential or cross-wake direction
$Z_w$	Zweifel load coefficient

### Greek:

$\beta$	Flow angle relative to axial direction
$\Gamma$	Circulation
$\eta$	Efficiency
$\tau$	Airfoil pitch
$\omega$	Vorticity
$\xi$	Total pressure loss coefficient

### Superscripts/Subscripts:

$+$	Wall units
$\infty$	Freestream
$o$	Degrees
$l$	Referenced to row inlet
$2$	Referenced to row exit
$abs$	Absolute reference frame
$pass$	Passage between airfoils
$rel$	Relative reference frame
$s$	Static conditions
$t$	Total (stagnation) conditions
$up$	Referenced to upstream conditions/location
$w$	Wake centerline
$x$	Axial direction

## FUNDAMENTAL STUDIES

Steady-state and time-resolved turbine flow fields were predicted using the 3-D RANS code described collectively by Ni [10], Ni and Bogoian [11], and Davis et al. [12]. Numerical closure for turbulence is obtained via the  $k-\omega$  model (Wilcox [13]) or the Baldwin Lomax [14] mixing length model. An O-H grid topology was employed with approximately 40,000 grid points per passage for two-dimensional simulations and approximately 600,000 grid points per passage for three-dimensional simulations without tip clearance. These grid counts provided essentially grid-independent solutions with values of  $y^+$  of the order 1 and approximately 7 grid points per momentum thickness. In steady mode the code is accurate to second-order in space, multi-grid techniques are used to obtain rapid convergence, and a mixing-plane model is employed at each inter-row boundary. To account for losses generated by the mixing of flow distortions, the exit flow field from each

row is circumferentially "mixed out" by a control-volume analysis that assumes a constant-area condition for the mixing process. The resulting 1D span-wise profiles are then passed into the downstream row. When run in time-accurate mode, the code employs implicit dual time stepping to solve for the periodic, unsteady flow field, and a sliding grid interface exists at inter-row boundaries. The code is accurate to second-order in space and time, and multi-grid techniques are used for the inner sub-iterations.

The results from simulations of wakes mixing under constant, and variable-area conditions are shown in Figure 1. The simulations were setup to simulate the experimental work of Hoffenberg and Sullivan [6] in which a flat plate was employed to generate a wake that was passed through a variable-area diffuser. Hoffenberg and Sullivan [6] considered only wake dilation (compression along the wake length) in their experimental study. As in their original report, the profiles shown in Figure 1 have been scaled by the velocity at the leading edge of the plate. The pertinent flow conditions were:  $Re_C=4.5 \times 10^6$ ,  $Tu_f=0.1\%$  and  $M_f=0.1$ . Here  $C$  refers to the plate length. It is convenient to introduce the Wake Velocity Ratio ( $WVR$ ), which is defined as:

$$WVR = \frac{V_2}{V_1} \quad (1)$$

where the right-hand side of Equation 1 is the ratio of the exit-to-inlet free-stream velocities related to the stream-wise distance over which the area change occurs. While a low-order parameter, it will be shown that  $WVR$  is useful for comparing geometrically simple cases with more complicated cases that, for example, include unsteady wake chopping as well as work extraction. Note that  $WVR$  is also called the de Haller coefficient [15] when used to indicate the velocity ratio across a passage in a compressor. A new term is adopted here because it is used with respect to the level of velocity variation, and hence dilation or contraction experienced by an airfoil wake *in its own frame of reference* as it propagates through a downstream blade row. By contrast, the de Haller number is used to indicate a velocity ratio across an airfoil row in the frame of reference of the local airfoil row.

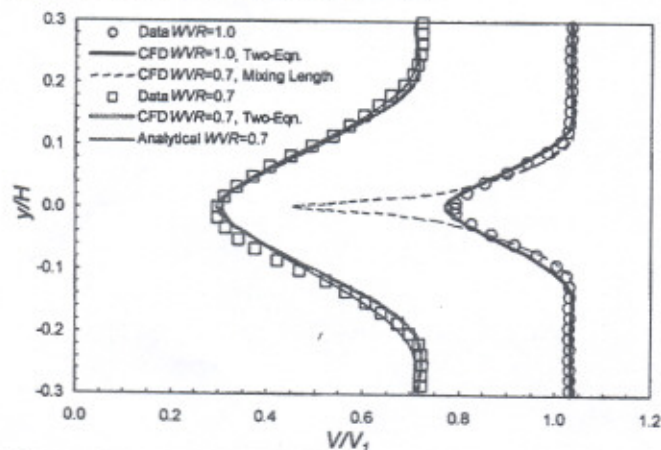


Figure 1. Comparisons of measured and predicted wake profiles exposed to constant- and variable-area mixing. Results for a  $WVR$  level of 0.7, analytically imposed on the predicted  $WVR=1.0$  wake shape, are also shown.

The constant-area mixing condition of Hoffenberg and Sullivan [6] was modeled with both the two-equation model

and the mixing-length model. The results plotted in Figure 1 show that the mixing-length model grossly over-predicts the peak velocity deficit in the wake. This is an inherent limitation of any mixing-length model because non-wall-bounded flows are modeled as laminar. As a result, the spreading/mixing rate of wakes is significantly under-predicted by mixing-length models. In contrast, the two-equation prediction more closely matches the data. The higher fidelity prediction from the two-equation turbulence model is primarily a result of the wake-mixing process being modeled as a turbulent one.

Simulation results for the  $WVR=0.7$  condition (increasing area) are also shown in Figure 1. Because of the low fidelity of the mixing-length model for wake flows, only the computational results from the two-equation turbulence model are shown for this condition. It is seen that the predicted wake profile for the compressed-wake condition matches the data from Hoffenberg and Sullivan [6] nearly as well as for the constant-area mixing condition. Most importantly though, the mixed-out loss of the compressed wake ( $WVR=0.7$ ), both measured and predicted, is 50% higher than that of the baseline wake exposed to constant-area mixing.

In order to isolate potential-field effects from viscous effects, the predicted wake-shape from the case with  $WVR=1.0$  was, by employing the Bernoulli and continuity equations, analytically exposed to an area increase equivalent to  $WVR=0.7$ . This process of taking the partially mixed constant-area ( $WVR=1.0$ ) wake profile from the exit and super-imposing a reduced  $WVR$  level assumes that the mixing process in the wake is minimally impacted by the pressure gradient. The results of this study, shown in Figure 1, demonstrate that the inviscid application of the pressure gradient causes the wake shape to be altered in a manner that matches the data nearly as well as the fully viscous simulation results also shown. This demonstrates that the dominant mechanism in wake-loss augmentation caused by flow divergence is an inviscid dilation of the stream tubes that comprise the wake. Van Zante et al. [3] drew a similar conclusion concerning the propagation of wakes through their compressor rig.

The numerical simulations of Hoffenberg and Sullivan [6], which employed two-equation and Reynolds-stress turbulence models, all matched the measured wake profiles essentially as well as the results presented here. Hoffenberg and Sullivan also found that if the area change applied to their wake was large enough, flow reversal, or wake bursting, occurred, and as a result wake characteristics became more difficult to accurately predict with CFD (Reynolds-Average Navier Stokes) simulations. Therefore, up to the point of wake bursting, CFD simulations, performed with at least the fidelity of a two-equation turbulence model, can provide reasonably accurate predictions of this phenomenon. Based on these results, controlled numerical experiments were conducted to identify the salient physical phenomena that govern wake mixing in turbomachines.

Figure 2 shows schematically the setup for a numerical study on the impact of flow-area changes on wake losses in compressible-flow regimes. A baseline wake was generated by passing flow over a NACA 0012 symmetric airfoil at zero incidence. Flow area was varied downstream of the airfoil by symmetric variation of the endwalls. Care was taken to ensure that the inlet (to the variable-area section) wake profiles were identical for all  $WVR$  levels considered. The span-wise dimensions in Figure 2 are exaggerated to show the shape of the endwalls. The actual inlet span for the calculations was set

at 0.02 cm with a slip boundary condition held for the endwalls. The dimension labeled  $s_{up}$  represents the stream-wise distance between the trailing-edge plane of the upstream row and the leading-edge plane of the downstream row while the dimension labeled  $s_{pass}$  represents the stream-wise distance within a downstream row passage. The flow conditions for the calculations were as follows:  $C_x=3.4\text{cm}$ ,  $Re_{C_x}=1.5 \times 10^5$ ,  $M_f=0.4$ ,  $s_{up}=1.3\text{cm}$ , and  $s_{pass}=3.4\text{cm}$ . These values approximate the stream-wise distances and flow conditions that exist in the LPTs of typical commercial engines, while the NACA 0012 airfoil represents the wake generating row and the endwalls impart the  $WVR$  of the downstream row in which the wakes mix. The chord of the NACA 0012 airfoil was scaled to provide a wake that approximated typical LPT wake characteristics at design conditions.

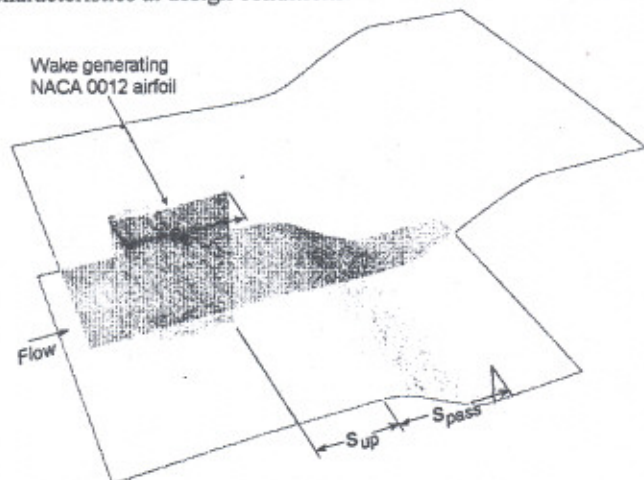


Figure 2. Schematic illustrating the setup for numerical study of wake mixing under variable-area conditions.

Figure 3 is a plot of wake-loss modification relative to the constant-area mixing case ( $WVR=1.0$ ) as a function of  $WVR$ . Here loss is defined as follows:

$$\xi = 100 \frac{(P_{11} - P_{12-MO})}{P_{11}} \quad (2)$$

where the pressures are mass averaged,  $MO$  indicates a mixed-out quantity, and stations 1 and 2 are taken at the inlet and exit to the diffuser section (labeled  $s_{pass}$  in Figure 2). Wake-loss modification is defined as the difference in wake-mixing loss between the  $WVR=1.0$  case and cases with  $WVR \neq 1.0$ . Note that the baseline wake-mixing loss for the  $WVR=1.0$  case in Figure 3 is 0.15. The results presented in this figure reveal that for  $WVR$  levels below 0.5, wake-mixing losses can increase as much as 100% or more above the baseline constant-area level. Also, the asymmetry of this plot about  $WVR=1.0$  indicates that wake loss augmentation ( $WVR < 1.0$ ) can be significantly more pronounced compared to wake-loss reductions ( $WVR > 1.0$ ). This asymmetry in wake-loss characteristic is consistent with results presented by Denton [5] and Rose and Harvey [8] based on analytically exposing an idealized square wake to a range of favorable and adverse pressure gradients. Finally, additional numerical studies revealed that the wake-loss behavior shown in Figure 3 is a weak function of Reynolds number.

One may note that the wake-loss augmentation for the case shown in Figure 1 with  $WVR=0.7$  is 50% above constant-area mixing loss, while the wake-loss augmentation for the same  $WVR$  level in Figure 3 is approximately 30%. The higher

wake-loss augmentation for the results shown in Figure 1 is a consequence of the area/velocity change being applied to the wake immediately at the trailing edge of the flat plate ( $s_{up}=0.0$  in Figure 2). The velocity gradients are highest in the wake near the trailing edge and little mixing loss has yet to be incurred. So, for a given  $WVR$  level, mixing-loss augmentation is highest when flow dilation is applied to a newly formed wake.

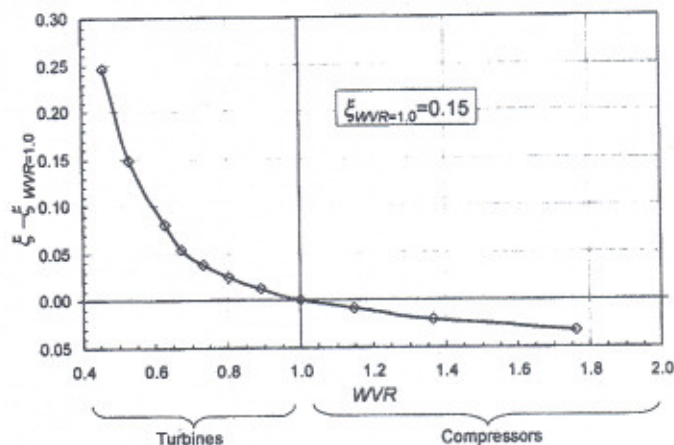


Figure 3. Wake-loss modification as a function of Wake Velocity Ratio ( $WVR$ ) for the endwall-variation simulations.

#### TURBINE-SPECIFIC APPLICATIONS

Up to now the discussion has concerned primarily the effects of wake compression achieved by the application of adverse pressure gradients, whereas turbine designers and analysts typically think of vanes and blades as flow accelerators in the local reference frame. The range of  $WVR < 1.0$  in Figure 3 is labeled "Turbines," based on results such as those shown in Figure 4. This figure shows instantaneous mid-span entropy distributions from a time-accurate simulation of an LPT. Time-mean wake-fluid trajectories (in the wake-generation reference frame) through the downstream row have been overlaid in this figure for clarity. Comparison of the flow area change (labels  $A_1$  and  $A_2$ ) between the two wake trajectories illustrates the dilation of the flow through the second row. In this case, the



Figure 4. Instantaneous entropy distributions with time-mean wake paths from a time-accurate simulation of an LPT.

flow dilation represents nearly an 80% increase in flow area and is imparted mainly by work being extracted from the flow by the second row in the wake-generation reference frame. No information has been given as to which row is the blade and which the vane in Figure 4 because the wake-trajectory behavior shown is the same regardless. That is to say, vane rows dilate blade wakes and blade rows dilate vane wakes.

While one normally analyzes the flow through a turbine passage in the frame of reference of the local airfoil, what is important in this context is the effect of the downstream airfoil on the wake in the frame of reference where the velocity defect was generated. In other words, because wake-mixing losses are generated by mixing between low- and high-momentum fluid streams in the vicinity of the wake, the wake-generation reference frame is the appropriate frame for analyzing this phenomenon. For example, consider the effect of downstream blades on the wakes from stationary vanes in the absolute frame. In Table 1, a portion of the velocity triangle data presented by Cherry and Dengler [16] for the GE E<sup>3</sup> LPT is given. For all five stages of the LPT, the flow accelerates through the vane row from an inlet Mach number of order 0.4 to an exit Mach number of order 0.6. Then, the flow passes through a downstream blade row with a consequent decrease in the absolute Mach number. Since each blade row extracts stagnation enthalpy from the flow, it follows that the blade row has decreased the local velocity substantially from the level obtained at the exit of the upstream vane. Similarly, if one considers the effect of a downstream vane row on the flow velocity exiting a blade row in the rotor-relative frame, the effect is the same: the vane row decelerates, or dilates the blade-exit flow in the rotating reference frame. So, the discussion of the effect of a diffuser on a wake velocity profile is indeed germane to the case of flow through a turbine.

**Table 1.** Inlet and exit Mach numbers for the GE E<sup>3</sup> LPT from Cherry and Dengler [16].

Stage	Vane $M_{2,abs}$	Blade $M_{1,rel}$	Blade $M_{2,rel}$	Blade $M_{2,abs}$
1	0.63	0.43	0.60	0.39
2	0.63	0.41	0.62	0.39
3	0.64	0.40	0.65	0.39
4	0.59	0.34	0.60	0.35
5	0.53	0.32	0.50	0.33

Smith [2] was the first to argue, on the basis of both potential flow theory and the energy equation, that a turbine blade row acts to increase the velocity defect across a wake emanating from an upstream vane. Adamczyk [17] and Greitzer et al. [4] have in turn discussed Smith's view of the physical process in more detail, and their arguments can be understood with reference to the two-dimensional flow depicted in Figure 5. Because the wake propagation through the blade passage is assumed inviscid, no fluid crosses the wake boundary as the wake convects. And, because the flow is also assumed incompressible, Kelvin's circulation theorem applies to a closed loop that passes through the wake centerline and the suction-side boundary of the velocity defect. Invoking Stokes' theorem, the flux of vorticity through the area enclosed by the loop remains constant as the wake propagates, and Equation 3 applies:

$$\Gamma = \iint \vec{n} \cdot \vec{\omega} \, dA = \iint |\vec{\omega}| \, dA \quad (3)$$

Since the area integral involves only the vorticity magnitude, which is in the span-wise direction for this 2-D flow, coordinate axes can be chosen arbitrarily along and normal to the axis of the wake centerline. Assuming the wakes are rectangular, as did Smith, and assuming that the velocity profile across the wake half width is linear (a rough approximation consistent with the wakes shown in Figure 1), gives:

$$\Gamma = \int_0^b \frac{V_\infty - V_w}{b} l \, dy = (V_\infty - V_w) l \quad (4)$$

In Equation 4,  $dy$  is an infinitesimal distance normal to the wake centerline,  $b$  is the wake half-width,  $l$  is the wake height, and  $V_\infty$  and  $V_w$  are the velocities at the edge of the wake and along the wake centerline, respectively. Applying Equation 4 at the two locations demarcated in Figure 5 gives:

$$(V_\infty - V_w)_2 = (V_\infty - V_w)_1 l_1 / l_2 \quad (5)$$

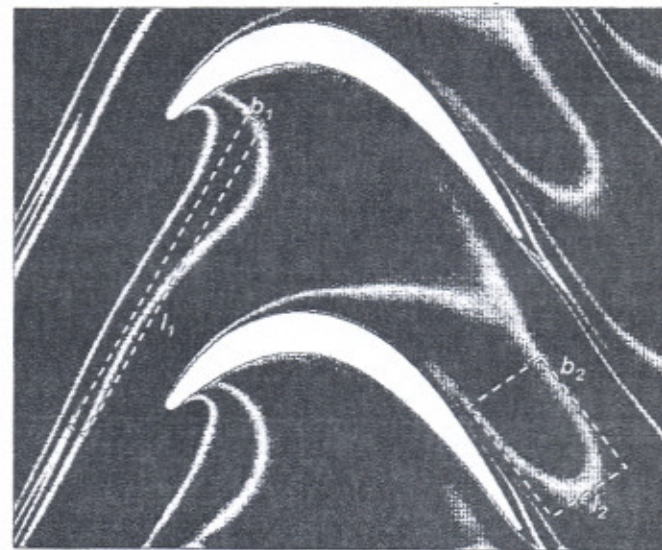


**Figure 5.** The development of a wake through a downstream row of airfoils. The idealized view of Smith [2] is shown applied to the wake half width.

So, as the streamlines converge through the turbine passage, the length of the wake segment subsequently decreases, and the velocity defect across the vane wake intensifies. The results of this simple analysis due to Smith are in keeping with the effects deduced by considering the propagation of a velocity defect through a diffuser. However, since the latter viewpoint suggests the simple correlating parameter of the *WVR*, it was adopted exclusively for the remainder of this work. This is not to say that the unsteady nature of the flow through a turbine row imparts an identical level of loss augmentation as the steady flow through a diffuser with the same *WVR* level. However, it will be demonstrated that loss increases engendered by both forms of flow dilation are essentially the same.

To study the details of wake mixing within downstream rows in turbines, two-dimensional "stages" were designed with systematically varied *WVR* levels for the second row. As illustrated in Figure 6, a flat plate was employed to generate moving wakes upstream of the vane row. For the plates, a five-to-one elliptical leading edge and circular trailing-edge shapes were employed while the plate thickness was set to match the trailing-edge thickness of typical commercial LPT airfoils. As

in the endwall study, the lengths of the wake-generating plates were scaled to provide wake profiles that approximated those from typical in-service LPTs at design conditions. The axial spacing between the two rows was initially set at half the axial chord of the second row, although subsequent simulations involved variable spacing in order to study that effect on wake-mixing losses.

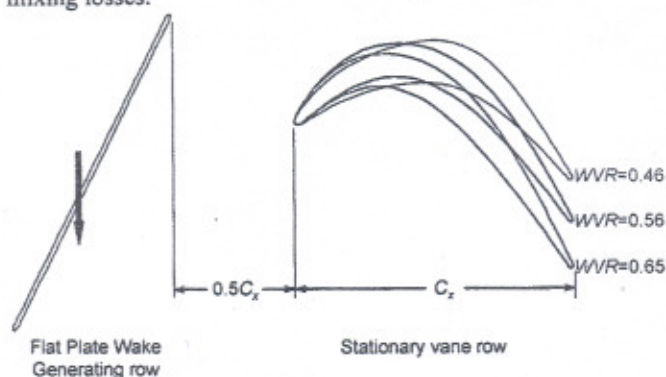


Figure 6. Schematic representation of the setup employed to study the mixing of wakes in a multi-row environment.

The variation of  $WVR$  for the stage calculations was accomplished by adjusting the design exit flow angle of the second row while maintaining the loading convention (e.g. front- versus aft-loaded) in three separate studies;

- 1) Holding the Zweifel load coefficients ( $Z_w$ ) constant for all three  $WVR$  levels and running with the second row as a vane (stationary).
- 2) Holding the Zweifel load coefficients constant and running with the second row as a blade (rotating).
- 3) Holding the airfoil pitch ( $\tau$ ) constant while allowing the Zweifel load coefficients to vary (second row as vane).

The primary design parameters of the second row for studies 1 and 2 are shown in Table 2. In the third, constant-pitch vane study, the pitch was held to the  $WVR=0.56$  level shown in Table 2. The inlet flow angle and Mach number were maintained for all of the stage simulations at 43.0 degrees and 0.4 respectively while the Reynolds number based on the vane axial chord was held at  $1.5 \times 10^5$ . Wake velocity ratio ( $WVR$ ) is defined here as the exit-to-inlet velocity ratio across the second row in the reference frame of the wake-generating row.

Table 2. Design parameters for the second row of the stage calculations. All dimensions are in cm.

	$\beta_1$	$\beta_2$	$C_x$	$\tau$	$Z_w$	Turning
$WVR=0.65$ :	43.0	59.0	2.54	2.49	1.26	$102^\circ$
$WVR=0.56$ :	43.0	56.8	2.54	2.25	1.26	$100^\circ$
$WVR=0.46$ :	43.0	52.0	2.54	1.96	1.26	$95^\circ$

The computational interface plane was placed midway between the two rows, or,  $0.25C_x$  upstream of the second row. The pitch of the wake-generating flat plates was set to match that of each airfoil design in order to simplify running of the time-resolved simulations. Consequently, for studies 1 and 2, wake-passing frequency varied (by approximately 10%) with each  $WVR$  level considered. For the third study, where the airfoils were redesigned to all have the same pitch, the Zweifel load coefficients varied by approximately 10% between designs. Finally, the wake shapes generated by the upstream

plates were compared for all stage calculations and found to be very nearly identical.

Each stage was first run in steady mode with the boundary layers modeled as fully turbulent and employing the mixing-plane model to transfer flow quantities between the two rows. In this mode, wakes do not pass into the second row; instead, they are mixed-out at the inter-row interface assuming a constant-area mixing condition. Each stage was also run in time-accurate mode with the boundary layers modeled as fully turbulent. The time-accurate simulations were performed with 100 time steps per cycle and 10 inner iterations per time step. The simulations required approximately 8 cycles to converge to a periodic solution.

Figure 7 is a plot of predicted row-loss augmentation levels as a function of  $WVR$  for the three stage studies performed. The term "row-loss augmentation" is used here instead of "wake-loss augmentation" because the losses presented in this figure also include variations in boundary-layer generated losses on the airfoil. Also included in Figure 7 is a plot of predicted wake-loss augmentation from a series of endwall-variation simulations such as that depicted in Figure 2. Surface-distances, Reynolds number, and inlet Mach number of the stage calculations were all matched for the endwall-variation simulation results shown in Figure 7. The initial (pre-dilation) wake profiles were also matched to those of the stage simulations by using the same wake-generating flat plate.

Row-loss augmentation was established for the stage calculations by subtracting the steady airfoil (second row) loss from the time-mean loss of the time-accurate simulation, where the two losses are defined as follows:

$$\xi_{ST} = 100 \frac{(P_{i1} - P_{i2-MO})}{P_{i1}} \quad (6)$$

$$\xi_{TA} = 100 \left( \frac{P_{i1} - P_{i2-MO}}{P_{i1}} \right) \quad (7)$$

In each relation  $MO$  indicates a mixed-out pressure, all other pressures are mass averaged, subscripts 1 and 2 denote the inlet and exit to the vane row respectively, and quantities in the relative reference frame of the second row were employed.

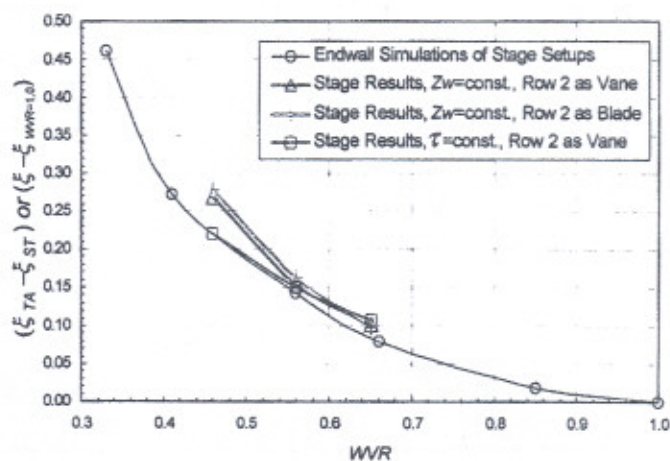


Figure 7. Loss augmentation as a function of  $WVR$  for endwall-variation and stage calculations.

The steady row losses,  $\xi_{ST}$ , obtained in the constant-loading stage calculations with  $WVR$  levels 0.46, 0.56, and 0.65 were 1.24, 1.50, and 1.66 percent, respectively. These loss levels,

taken together with the results shown in Figure 7, indicate that row losses were increased by 6 to 22 percent for the  $WVR$  levels considered here. Time-mean suction-side boundary layer momentum deficits were compared to the result from the steady simulations and found to experience no more than a 7% increase. Variations of the pressure-side boundary layer parameters between steady and time-averaged time-accurate results were comparatively negligible. Considering the fractional contribution of the suction-side boundary layers to the total row loss, a maximum loss contribution of 0.04 percent is attributable to increased boundary-layer loss. Also, a comparison of steady and time-mean wall-shear distributions revealed variations of less than 5% over the airfoil surface.

The results for the three stage studies (constant-loading vane, constant-loading blade, and constant-pitch vane) shown in Figure 7 reveal similar trends and loss-augmentation levels. These results support the thesis that flow dilation within the downstream row, caused by work extraction in the wake-generating reference frame, results in enhanced mixing losses. This phenomenon occurs for *both* vane wakes passing through blade rows and blade wakes passing through vane rows.

Additionally, the results shown in Figure 7 from the three stage studies also exhibit the same trend and similar loss-augmentation levels as the results from the endwall-variation simulations. This agreement in wake/row-loss augmentation between the stage and endwall-variation simulations demonstrates that, although the unsteady kinematics of wake chopping and advection present in the stage calculations appear complicated, wake-mixing loss is primarily affected by the gross flow dilation or contraction imparted by the row of downstream airfoils.

In Figure 8 the steady and time-averaged entropy distributions for each  $WVR$  level considered in the stage study with constant-loading vanes are shown. The entropy increase relative to the inlet state was calculated using Gibbs' equation at each computational node for each time step, and the results were then time-averaged. In the time-averaged distributions, a region of elevated entropy (relative to the steady results), biased to the suction-side of the passage, is evident for all three  $WVR$  levels. Hodson and Dawes [7] reported a similar augmentation of measured loss levels on the suction side of a cascade passage when unsteady wakes were introduced. This region of elevated entropy was reportedly linked to wake fluid migrating toward the suction side of the passage as the chopped wake segments were convected through the passages.

For all three  $WVR$  levels shown in Figure 8, the time-mean entropy elevation begins just downstream of the leading-edge plane of the passages. This is consistent with the wake fluid responding to an increase in flow area imparted by the second row (a vane in this case) as it begins to turn the fluid. Entropy can be seen to accumulate through the passage (just above the suction-side boundary layer) until the trailing edge, after which the entropy levels remain relatively constant with axial distance. This trend is consistent with flow dilation taking place only within the passage as the flow is turned by the downstream row. As a last note related to Figure 8, time-mean entropy distributions for the constant-loading blade and constant-pitch vane studies were similar to those shown in Figure 8.

Figure 9 shows time-mean wake paths (in the wake reference frame) superimposed on instantaneous distributions of entropy for the time-accurate simulation with  $WVR=0.56$  from the constant-loading vane study. It can be seen from the

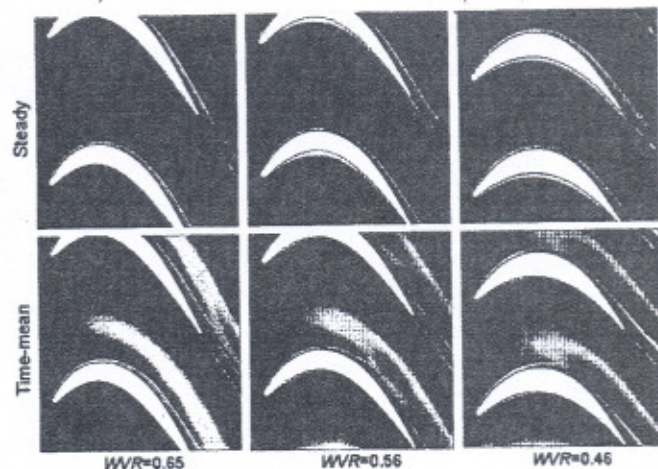


Figure 8. Comparisons of steady and time-mean entropy distributions from the constant-loading stage simulations.

wake paths that the wake fluid begins to turn immediately upon entering the passage of the second row. The accumulation of wake fluid on the suction side is evident in this figure and is consistent with the results presented in Figure 7. This phenomenon of wake fluid migration toward the suction side of the passage is also consistent with the experimental and computational works of Hodson and Dawes [7], Korakianitis [18], and Stieger and Hodson [19] for turbine-specific configurations.

As mentioned previously, Rose and Harvey [8] developed a model for predicting wake-mixing losses that included the effects of passing through blade rows. They validated their model by comparing their predicted trends to results from a time-accurate CFD prediction of a vane wake passing through a blade row at a single instant in time. Comparisons were made to instantaneous mid-span, pitch-wise distributions of entropy at the inlet and exit of the blade row. In Figure 9 two instants in time for which one could compare inlet and exit pitch-wise entropy distributions across this airfoil row are indicated by  $t_1$  and  $t_2$  (i.e. if one considers small changes in time to translate to small variations in distance). The pitch-wise averaged entropy at  $t_1$  is found to be significantly higher than at  $t_2$  because a segment of wake fluid is included in the  $t_1$  average and not in the  $t_2$  average. In fact, the instantaneous loss across the airfoil row shown in Figure 9 experiences a minimum that is negative,



Figure 9. Instantaneous entropy distributions with superimposed time-mean wake paths (in the wake-generation reference frame) for the stage simulation with  $WVR=0.56$ .

while the peak instantaneous loss level is more than two times the time-mean level. So, because wakes are segmented by the downstream row, a variety of conclusions might be drawn concerning wake-mixing behavior in downstream rows if the entropy change across the downstream row is evaluated in an *instantaneous* sense. Also, the CFD code utilized by Rose and Harvey employed a mixing-length turbulence model, a class of turbulence model which was earlier shown (Figure 1) to be particularly deficient in predictive capabilities for wake flows.

For the constant-loading vane case with  $WVR=0.56$ , the inter-row stream-wise distance,  $s_{up}$ , was varied to investigate its effect on wake mixing in a multi-row environment. For this study, the row interface plane (mixing plane in the steady simulations) was maintained at  $0.25C_x$  upstream of the vane leading edge. Figure 10 is a plot of row-loss augmentation as a function of  $s_{up}$ . One can see from this figure that row-loss augmentation can be decreased dramatically with increased  $s_{up}$ . The reduction in row-loss augmentation with increased  $s_{up}$  is primarily a result of additional (relative to the baseline case with  $s_{up}=0.5C_x$ ) mixing of the wakes occurring before entering the vane row. On the other hand, Figure 10 demonstrates that as  $s_{up}$  is decreased, row-loss augmentation increases because the wakes are less mixed upon entering the downstream row. This is of course opposite the trend typically reported for subsonic compressors [3, 4].

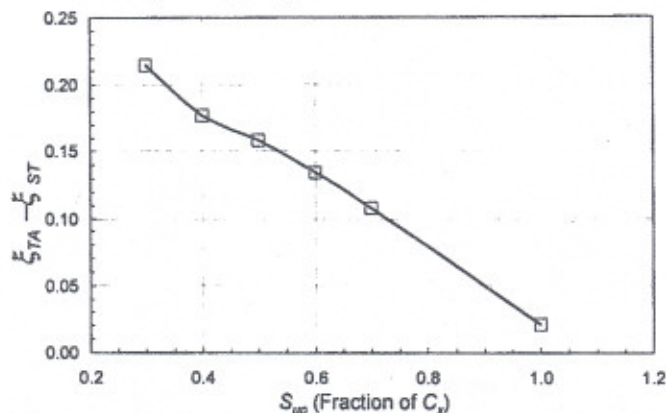


Figure 10. Row-loss augmentation as a function of stream-wise distance between stage rows.

To investigate if the airfoil loading convention, i.e. front or aft loading, plays an important role in the mixing of wakes in turbines, the airfoil with  $WVR=0.56$  was redesigned to be distinctly front loaded. The row-loss augmentation for the front loaded airfoil was predicted to be minimally higher (0.01%) than for the original design. This is consistent with the concept that a less mixed-out wake will realize a larger loss augmentation for a given level of  $WVR$  because the front loaded design turns the flow earlier in the passage than the original design, where the incoming wakes are less mixed.

In summary, it has been demonstrated that the first order parameter governing wake-loss modification in axial-flow turbines and compressors is the gross level of velocity change imparted by the row of downstream airfoils. Quantification of the gross velocity change, or  $WVR$ , of the downstream row can only be realized by considering the velocity gradient across that row in the wake-generation reference frame. However, the results presented here demonstrate that wake-loss augmentation in turbines is not only a function of  $WVR$ . Two additional key parameters that govern how a wake mixes in a downstream row

are the state of mixing of the wake as it enters the downstream row, as well as the stream-wise distance over which the velocity decrease due to work extraction occurs.

As the effects of wake-loss augmentation have not been quantified for practical applications, the following section attempts to illustrate the impact of this phenomenon on the performance of LPTs through the use of rig data and simulations.

## ENGINE APPLICATIONS

Evaluation of LPT rig efficiency data in the context of wake-mixing losses is shown in Figure 11. The data and time-accurate simulation results are the same as those presented as "Rig B" results in Praisner et al. [9] with the addition here of the steady simulation results. The transition-modeling capability reported by Praisner and Clark [20] and Praisner et al. [9] was employed for these rig simulations. Use of a transition modeling capability is important here because it allows for useful comparisons to be made with the data (absolute values), which are from a rig run at conditions where the boundary layers cannot be considered fully turbulent. Also, although these simulations were performed with transition modeling, there were no suction-side boundary layer separations, and hence, one would not expect wetted losses to change appreciably between steady and time-accurate conditions as a result. Finally, it should be noted that the simulation results presented here included simplified geometric modeling of the endwalls, which results in the over-prediction of efficiency levels at the extreme span-wise locations.

The time-mean results from the time-accurate simulation shown in Figure 11 provide more accurate prediction of efficiency levels between approximately 5 and 95 percent span compared to the steady simulation. Similar to the results presented by Praisner et al. [9], the predicted integrated efficiency drops 0.8% between the steady and time-accurate simulations for this rig. This level of efficiency drop is present even at mid-span, well away from endwall effects. Comparisons of steady and time-mean boundary layer parameters revealed small variations, again indicating that a mechanism for core-flow loss enhancement was at the root of the difference. In Figure 11 it can also be seen that the efficiency lost to unsteadiness is highest in the span-wise regions between 5 and 25 percent and 75 and 90 percent span. This is thought to be a result of: 1) span-wise mixing being

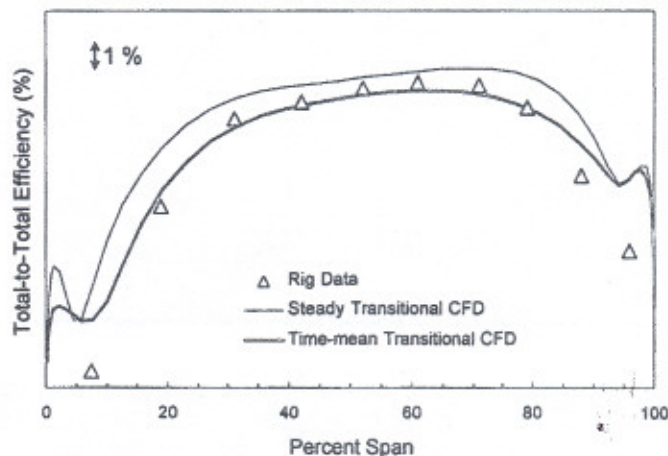


Figure 11. Efficiency-versus-span data with steady and time-accurate transitional CFD predictions for an LPT rig.

more accurately captured in the time-accurate simulation, and 2) the greater fraction of the flow occupied by distortions, such as the passage vortices generated in endwall regions (see Payne et al. [21] and Walraevens and Gallus [22]).

While the LPT presented in Figure 11 realized a 0.8% efficiency debit attributable primarily to enhanced wake-mixing losses, other LPT designs have been found to produce as much as a 1.5% drop in efficiency associated with enhanced wake-mixing losses. As in the results reported in Figure 11, for the case with a 1.5% efficiency drop the time-resolved simulation was the most accurate. It is worth noting that this large loss in efficiency is attributable to incremental loss increases in each row (due to mixing loss enhancements) across the numerous rows (up to 14) that comprise an LPT. Since efficiency degradation due to wake-loss enhancement is roughly proportional to the number of airfoil rows, one might expect it to be significantly smaller for high-pressure turbines.

Figure 12 is a plot of predicted row-loss augmentation (as defined by Equations 6 and 7) compared with  $WVR$  levels for two embedded stages of an LPT rig. Comparison of the  $WVR$  levels and wake-loss augmentation between rows is only valid here because the Mach numbers and stream-wise distances between rows are essentially the same for the four rows considered. In Figure 12 the inverse relationship between  $WVR$  and row-loss augmentation is clearly evident. However, more importantly, the losses of each vane and blade row increase as a result of enhanced wake-mixing losses. This is consistent with the stage-simulation results presented in the previous section in which both vane and blade rows were shown to increase the mixing losses of wakes passing through them.

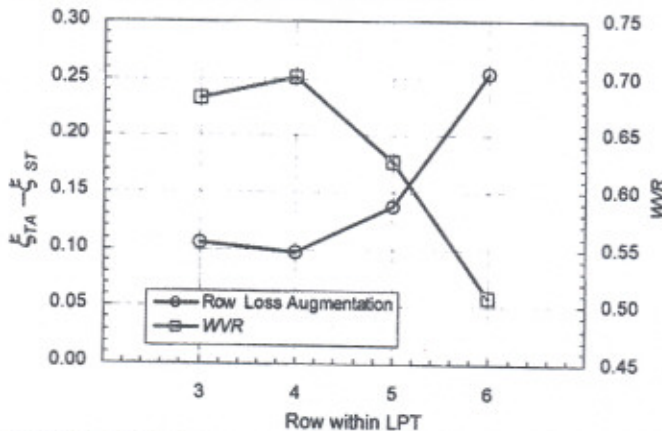


Figure 12. Row-loss augmentation compared to  $WVR$  levels for four rows of an LPT.

As the Mach numbers and stream-wise distances of the stage-simulations (Figure 7) are similar, by design, to those in the rig considered in Figure 12, a comparison of loss augmentation levels between the two is presented in Table 3. Here a least-squares fit of the stage-simulation results was employed to interpolate the results between Figures 7 and 12. From Table 3 it is clear that the row-loss augmentation levels and trend from the rig simulation are in good agreement with the wake-loss augmentation levels and trend shown in Figure 7. The systemically higher row-loss augmentation levels realized in the rig simulation are thought to be primarily a result of the larger level of flow distortions (wakes plus passage vortices, endwall boundary layers, etc.) per passage in the three-

dimensional simulation compared to the two-dimensional simulations that capture only wakes. That is to say, any velocity gradient, whether it comprises a vortex sheet such as a wake, or a passage vortex generated in an endwall region, will experience increased mixing losses when convecting through a downstream row in a turbine.

Table 3. Comparison of rig and stage-calculation row-loss augmentation levels for each row of the rig.

	Stage Simulations	Rig simulation
Row 3, $WVR=0.69$	0.09%	0.11%
Row 4, $WVR=0.70$	0.09%	0.10%
Row 5, $WVR=0.63$	0.12%	0.14%
Row 6, $WVR=0.51$	0.21%	0.25%

## CONCLUSIONS

An investigation has been conducted into the behavior of wakes mixing through downstream rows in turbomachines. Basic experimental data, analytical and numerical studies, and low-pressure turbine rig data were employed to study the phenomenon of wake mixing in downstream rows. It was shown that the dominant mechanism in the alteration of wake mixing caused by free-stream velocity changes is an inviscid dilation or contraction of stream tubes. The simulation code employed in this study has been shown to capture this effect with a good degree of accuracy by comparison to experimental data. Numerical studies of realistic wake profiles revealed that the detrimental effects of wake dilation on wake-mixing losses are significantly more pronounced than the benefits of wake recovery engendered by wake contraction.

Experimental and numerical results have been presented which demonstrate that in turbines, wakes are diluted within the immediate downstream row, be it a blade or a vane. A simple parameter, the wake velocity ratio, has been employed to isolate the effects of downstream rows on the wake-mixing process. Additionally, the loading convention of the downstream row has been shown to be of secondary importance in determining the impact of downstream-row geometry on wake losses. A more dominant geometric parameter is the stream-wise distance between rows: larger stream-wise distance results in better performance because the wakes mix more before they experience the dilation imparted by the downstream row. Additionally, comparisons between rig data and simulations indicate that dilation of flow distortions, such as wakes and endwall vortices, can contribute up to 1.5 percent of lost efficiency in low-pressure turbines.

Future work might include the development of a reduced-order model of wake-loss augmentation for implementation in preliminary design methods such as meanline predictive tools or for modification of a mixing-plane formulation in steady CFD simulations.

## ACKNOWLEDGMENTS

The authors would like to thank Pratt & Whitney for permission to publish this work. More specifically, the support and encouragement of Joel Wagner, Richard Gacek, Francis Price, Shankar Magge and Gary Stetson is greatly appreciated. The authors would also like to acknowledge the thorough and constructive comments provided by the reviewers.

## REFERENCES

- [1] Hill, P. G., Schaub, U. W., and Y. Senoo, 1963, "Turbulent Wakes in Pressure Gradients," *Journal of Applied Mechanics*.

- [2] Smith, L. H., 1966, "Wake Dispersion in Turbomachines," ASME Journal of Basic Engineering, Vol. 88, No. 3.
- [3] Van Zante, D. E., Adamczyk, J. J., Strazisar, A. J., and Okiishi, T. H., 2002, "Wake Recovery Performance Benefit in a High-Speed Axial Compressor," ASME Journal of Turbomachinery, Vol. 124.
- [4] Greitzer, E. M., Tan C. S., and Graf, M. B., 2004, Internal Flows: Concepts and Applications, Cambridge University Press, Cambridge, U.K.
- [5] Denton, J. D., 1993, "Loss Mechanisms in Turbomachines," ASME Journal of Turbomachinery, Vol. 115.
- [6] Hoffenberg, R., Sullivan, J. P., 1998, "Measurement and Simulation of Wake Deceleration", AIAA-1998-522.
- [7] Hodson, H. P., Dawes, W. N., 1998, "On the Interpretation of Measured Profile Losses in Unsteady Wake-Turbine Blade Interaction Studies," ASME J. of Turbomachinery, Vol. 120.
- [8] Rose, M. G., Harvey, N. W., 1999, "Turbomachinery Wakes: Differential Work and Mixing Losses", ASME Paper 99-GT-25.
- [9] Praisner, T. J., Grover, E. A., Rice, M. J., and Clark, J. P., 2004, "Predicting Transition in Turbomachinery, Part II - Model Validation and Benchmarking," ASME Paper GT-2004-54109.
- [10] Ni, R. H., 1982, "A Multiple-Grid Scheme for Solving the Euler Equations," AIAA Journal, Vol. 20, No. 11, pp. 1565-1571.
- [11] Ni, R. H. and Bogoian, J. C., 1989, "Prediction of 3-D Multistage Turbine Flowfield Using a Multiple-Grid Euler Solver," AIAA Paper 89-0203.
- [12] Davis, R.L., Shang, T., Buteau, J, and Ni, R.H., 1996, "Prediction of 3-D Unsteady Flow in Multi-Stage Turbomachinery Using an Implicit Dual Time-Step Approach," AIAA Paper 96-2565.
- [13] Wilcox, D.C., 1998, Turbulence Modeling for CFD, Second Edition, DCW Industries, Inc., La Canada, California.
- [14] Baldwin, B. S. and Lomax, H., 1978 "Thin-Layer Approximations and Algebraic Model for Separated Turbulent Flows," AIAA Paper 78-257.
- [15] Cumpsty, N. A., 1989, "Compressor Aerodynamics," Longman Scientific and Technical, Essex, U.K.
- [16] Cherry, D. G. and Dengler, R. P., 1984, "The Aerodynamic Design and Performance of the NASA/GE E3 Low Pressure Turbine," AIAA Paper 1984-1126.
- [17] Adamczyk, J. J., 2000, "Aerodynamic Analysis of Multistage Turbomachinery Flows in Support of Aerodynamic Design," ASME Journal of Turbomachinery, Vol. 122.
- [18] Korakianitis, T., 1993, "On the Propagation of Viscous Wakes and Potential Flow in Axial-Turbine Cascades," Transactions of the ASME, Journal of Turbomachinery, Vol 115.
- [19] Stieger, R. D., and Hodson, H. P., 2004, "The Unsteady Development of a Turbulent Wake Through a Downstream Low-Pressure Turbine Blade Passage," ASME Paper GT-2004-53061.
- [20] Praisner, T. J., and Clark, J. P., 2004, "Predicting Transition in Turbomachinery, Part I - A Review and New Model Development," ASME Paper GT-2004-54108.
- [21] Payne, S. J., Ainsworth, R. W., Miller, R. J., Moss, R. W., 2003, "Unsteady Loss in a High Pressure Turbine Stage. Part I: Time-mean Results," International Journal of Heat & Fluid Flow, 24.
- [22] Walraevens R. E., Gallus H. E., 1995, "Stator-Rotor-Stator Interaction in an Axial Flow Turbine and its Influence on Loss Mechanisms," AGARD PEP 85th Symposium, CP-571.